

Photon cooling: linear vs nonlinear interactions

A. Hovhannisyanyan¹, V. Stepanyan² and A.E. Allahverdyan³

¹*Institute of Applied Problems of Physics, Yerevan, Armenia*

²*Physics Department, Yerevan State University, Yerevan, Armenia*

³*Alikhanian National Laboratory (Yerevan Physics Institute), Yerevan Armenia*

Linear optics imposes a relation that is more general than the second law of thermodynamics: For modes undergoing a linear evolution, the full mean occupation number (i.e. photon number for optical modes) does not decrease, provided that the evolution starts from a diagonal state. This relation connects to noise-increasing (or heating), and is akin to the second law, though for the linear evolution it holds for a wider set of initial states. We show that this general trend can be reversed via nonlinear interactions between the modes. They can cool—i.e. decrease the full mean occupation number and the related noise—an equilibrium system of modes provided that their frequencies are different. Such an effect cannot exist in energy cooling, where only a part of an equilibrium system is cooled. We describe the cooling set-up via both efficiency and coefficient of performance, and relate the cooling effect to the Manley-Rowe theorem in nonlinear optics.

Cooling is needed for noise-reduction and for capturing quantum degrees of freedom. It has been studied during the past 100 years in various set-ups [1, 2]. Cooling processes are also fundamental for thermodynamics: they sharpen the understanding of the second law, and are instrumental for the third law [3]. An interesting example of this is the laser cooling of solids via the anti-Stokes effect, which does have both quantum and thermodynamic nature [1]. Much attention is currently devoted to cooling processes in quantum thermodynamics [4–19]. It is known that only a part of a thermally isolated (initially equilibrium) system can be cooled in terms of energy (or temperature), that cooling such systems costs high-graded energy (work), hence the definition of the coefficient of performance (COP), and that cooling is limited by energy spectra and complexity costs.

Here we consider bosonic (for clarity photonic) degrees of freedom (modes), and show that linear transformations (e.g. linear optics) always increase the full photon number of the system. This statement is akin to the second law, but in the linear regime it is more general, since it holds for a wider class of initial states. For such states increasing the mean photon number relates to increasing of noise (heating). This general trend in increasing the mean photon number can be reversed by nonlinear interactions. One can cool in this sense an initially *equilibrium* system, which consists of two or higher number of modes. This is not possible for energy cooling, where as demanded by the second law, only subsystem's energy can be decreased (cooled).

Our cooling set-up is characterized by two efficiency-like parameters: the coefficient of performance (COP) and the efficiency. The former refers to energy costs of cooling, while the latter normalizes the cooling result over the total changes introduced in the system. Nonlinear interactions achieve cooling in near-resonance regimes, where there is an effective conservation law in the number of photons (Manley-Rowe theorem) [20, 21]. Thus, this cooling scenario uncovers a thermodynamic role of

nonlinear optical processes. We work in terms of photons, but our results hold for other bosons (e.g. phonons).

No cooling for linear interactions. Linear processes describe the lion's share of boson dynamics [22, 23]. Consider a single mode that underwent a linear evolution governed by a quadratic Hamiltonian. In the Heisenberg picture, the general form of this evolution connects initial $a = a(0)$ and final $b = a(t)$ annihilation operator of the mode:

$$b = Sa + Ra^\dagger + f, \quad (1)$$

where S , R and f are complex c -numbers that characterize the evolution. The initial state (density matrix) ρ of the mode is diagonal in the representation of the initial occupation number $a^\dagger a$: $\langle a \rangle \equiv \text{tr}(a\rho) = \langle a^\dagger \rangle = 0$. The commutation relation $[b, b^\dagger] = [a, a^\dagger] = 1$ impose $|S|^2 - |R|^2 = 1$ in (1). Then we get from (1)

$$\langle b^\dagger b \rangle - \langle a^\dagger a \rangle = 2|R|^2 \langle a^\dagger a \rangle + |R|^2 + |f|^2 \geq 0, \quad (2)$$

i.e. the mean photon number difference defined in the LHS of (2) can only increase. In particular, this conclusion holds for linear amplifiers [22]. According to (1) also the dispersion of the photon number increases: $\langle (b^\dagger b)^2 \rangle - \langle b^\dagger b \rangle^2 \geq \langle (a^\dagger a)^2 \rangle - \langle a^\dagger a \rangle^2$. The analogue of (1, 2) for a fermion mode does not generally hold.

Importantly, (2) extends to the completely general N -mode situation, where instead of (1) we write

$$b_i = \sum_{j=1}^N (S_{ij}a_j + R_{ij}a_j^\dagger) + f_i, \quad i = 1, \dots, N, \quad (3)$$

where S_{ij} , R_{ij} and f_i are c -numbers; cf. (1)). Write (3) in block-matrix form:

$$\begin{pmatrix} b \\ b^\dagger \end{pmatrix} = E \begin{pmatrix} a \\ a^\dagger \end{pmatrix} + \begin{pmatrix} f \\ f^* \end{pmatrix}, \quad E = \begin{pmatrix} S & R \\ R^* & S^* \end{pmatrix}, \quad (4)$$

where $a = (a_1, \dots, a_N)^T$, a^\dagger , b , b^\dagger , f , and f^* are N -columns, and where T and * denote (resp.) transposition

and complex conjugation. Now commutation relations $[b_i, b_j^\dagger] = [a_i, a_j^\dagger] = \delta_{ij}$, where δ_{ij} is the Kronecker's delta, and $[b_i, b_k] = [a_i, a_k] = 0$ lead from (4) to (resp.):

$$SS^\dagger - RR^\dagger = I, \quad SR^T = RS^T, \quad (5)$$

where I is the $N \times N$ unit matrix. Eqs. (5) imply

$$E^{-1} = \begin{pmatrix} S^\dagger & -R^T \\ -R^T & S^T \end{pmatrix}. \quad (6)$$

The reasoning that led to (5) is now applied to (6), since the same commutation relations hold. Then we get in addition to (5) the following new relations:

$$S^\dagger S - R^T R^* = I, \quad S^\dagger R = R^T S^*. \quad (7)$$

Now assume that the initial state ρ of N modes holds:

$$\langle a_i^\dagger a_j \rangle \equiv \text{tr}(\rho a_i^\dagger a_j) = \delta_{ij} \langle a_i^\dagger a_i \rangle, \quad \langle a_i a_j \rangle = \langle a_j \rangle = 0, \quad (8)$$

where $i, j = 1, \dots, N$; e.g. (8) refers to initially independent modes in diagonal states. The initial state ρ that holds (8) need not be independent. Using (8) and the first equation in (7) we find for the change of the total occupation number:

$$\begin{aligned} \sum_{i=1}^N \left(\langle b_i^\dagger b_i \rangle - \langle a_i^\dagger a_i \rangle \right) &= \sum_{i=1}^N |f_n|^2 \\ &+ \sum_{i,j=1}^N (2 \langle a_i^\dagger a_i \rangle + 1) |R_{ij}|^2 \geq 0. \end{aligned} \quad (9)$$

Thus the full mean photon number can only increase under linear evolution [24]. This relation is akin to the second law, but for the linear evolution it is even stronger, since it holds for a more general class (8) of (non-equilibrium) initial states. For the particular case of Gaussian initial states, (9) follows from the result of Ref. [25] on the maximal work. Note that the analogue of (9) for energy does not hold, i.e. $\sum_{i=1}^N \omega_i \left(\langle b_i^\dagger b_i \rangle - \langle a_i^\dagger a_i \rangle \right)$ need not have a definite sign. Eq. (3) can describe absorption (attenuation) of photons from a few selection target modes, at the expense of their overall increase.

Eq. (9) can be interpreted as uncertainty increase. Indeed, $\langle a^\dagger a \rangle$ characterizes the dispersion $\langle \Delta a^2 \rangle$ of a [22]:

$$\begin{aligned} \langle \Delta a^2 \rangle &\equiv \frac{1}{2} \langle a a^\dagger + a^\dagger a \rangle - |\langle a \rangle|^2 = \langle a^\dagger a \rangle + \frac{1}{2} - |\langle a \rangle|^2 \quad (10) \\ &= \langle x^2 \rangle - \langle x \rangle^2 + \langle y^2 \rangle - \langle y \rangle^2, \quad a = x + iy, \end{aligned} \quad (11)$$

where $x = (a + a^\dagger)/2$ and y are Hermitian operators. Eq. (10) is the definition of dispersion for non-hermitian a , while (11) shows how it can be measured via its Hermitian components x and y . For considered initial states (8), Eqs. (9–11) imply that also the sum of uncertainties (10) increases and not just the photon number. In all scenarios we consider, cooling will simultaneously mean the uncertainty decrease in the sense of (10). Note that $\langle a^\dagger a \rangle$ also controls the shot noise in photodetection [23].

Cooling two equilibrium modes. Once (9) is understood, it is natural to ask whether non-linear processes can cool, i.e. decrease the initial number of photons. To facilitate the thermodynamic meaning of this question, we shall consider two initially Gibbsian equilibrium bosonic modes at the same temperature T . Now a single equilibrium mode cannot be cooled by any unitary (generally nonlinear) operation, since the mean occupation number is proportional to the energy, and the energy decrease for such a situation is prohibited by the second law. However, two initially equilibrium modes at different frequencies can be cooled, in terms of the mean full occupation number, via specific non-linear interactions. Hence, we shall first determine the optimal cooling, and then turn to non-optimal but feasible scenario from the viewpoint of experimentally realizable nonlinear interactions. Consider the initial state of two modes with frequencies ω_1 and ω_2 at temperature T :

$$\rho = \xi e^{-\beta \sum_{i=1}^2 \omega_i \hat{n}_i}, \quad \xi = (1 - e^{-\beta \omega_1})(1 - e^{-\beta \omega_2}), \quad (12)$$

$$\hat{n}_i \equiv a_i^\dagger a_i, \quad i = 1, 2, \quad \hat{n} \equiv \sum_{i=1}^2 a_i^\dagger a_i, \quad (13)$$

where $\hbar = 1$, $\beta = 1/(k_B T)$ and \hat{n}_i are the occupation number operator for each mode. The two-mode system undergoes a unitary process that aims at cooling:

$$\rho(t) = U \rho U^\dagger, \quad U U^\dagger = 1. \quad (14)$$

COP and efficiency. Besides targeting the mean occupation number, we characterize the cooling via two efficiency-like quantities. Since ρ in (12) is an equilibrium state, the final average energy found from (14) is larger than the initial one, which is the second law:

$$\sum_{i=1}^2 \omega_i \Delta n_i \geq 0, \quad \Delta n_i \equiv \text{tr}(\rho[U^\dagger \hat{n}_i U - \hat{n}_i]). \quad (15)$$

Eq. (15) defines the energy cost of cooling and it motivates the usual definition of coefficient of performance (COP) [19], where the achieved cooling $-\sum_{i=1}^2 \Delta n_i > 0$ is divided over the energy cost $\sum_{i=1}^2 \omega_i \Delta n_i$. We use the dimensionless COP conventionally defined as:

$$K = -\frac{\Delta n_1 + \Delta n_2}{\Delta n_1 + \alpha \Delta n_2}, \quad \alpha \equiv \frac{\omega_2}{\omega_1} < 1, \quad (16)$$

where a larger K means e.g. a better cooling with a smaller energy cost. In (16) we took $\alpha < 1$ without loss of generality. Hence, the fact of cooling $-\sum_{i=1}^2 \Delta n_i > 0$ implies via (15) and $\alpha < 1$

$$0 \leq \alpha(-\Delta n_2) \leq \Delta n_1 \leq (-\Delta n_2). \quad (17)$$

Now (17) motivates us to define $\Delta n_1 - \Delta n_2 = |\Delta n_1| + |\Delta n_2|$ as the total number of occupation changes introduced in the system. This is consistent with thinking about the cooling as photon conversion: some amount of low energy photons ($\Delta n_2 < 0$) transform into a smaller

amount of higher energy photons ($\Delta n_1 > 0$). The sum of low energy photons given and high energy photons received will be the total number of occupation changes. Only a fraction η of those lead to cooling:

$$\eta = -\frac{\Delta n_1 + \Delta n_2}{\Delta n_1 - \Delta n_2}. \quad (18)$$

We call η the efficiency of cooling. It is similar to other quantum efficiencies employed in optics. Using (15, 17) we get a Carnot-type bound where temperatures are replaced by frequencies:

$$\eta \leq \frac{\Delta n_1 + \Delta n_2}{\Delta n_2} \leq 1 - \frac{\min[\omega_1, \omega_2]}{\max[\omega_1, \omega_2]}, \quad (19)$$

i.e. cooling is impossible for $\omega_1 = \omega_2$.

Optimal cooling. Given (14,13), we look for the unitary which minimizes the mean of \hat{n} in the final state:

$$U_{\text{opt}} = \text{argmin}_U [\text{tr}(U\rho U^\dagger \hat{n})], \quad (20)$$

Noting the eigenresolutions [cf. (12, 13)]

$$\rho = \sum_{k=0}^{\infty} r_k |r_k\rangle \langle r_k|, \quad \hat{n} = \sum_{l=0}^{\infty} \nu_l |\nu_l\rangle \langle \nu_l|, \quad (21)$$

we get from (14, 21, 20)

$$\text{tr}(U\rho U^\dagger \hat{n}) = \sum_{k,l=0}^{\infty} r_k \nu_l z_{kl}, \quad z_{kl} = |\langle \nu_l | U | r_k \rangle|^2, \quad (22)$$

where $\sum_k z_{kl} = \sum_l z_{kl} = 1$, i.e. z_{km} is a doubly stochastic matrix. Such matrices form a compact convex set with vertices being permutation matrices [26]. As (22) is linear from z_{km} it reaches the minimum value on the vertices. Thus U_{opt} is a permutation matrix, and its form is seen from (22, 21):

$$\text{min}_U [\text{tr}(U\rho U^\dagger \hat{n})] = \sum_{k=0}^{\infty} \nu_k^\uparrow r_k^\downarrow, \quad (23)$$

$$\nu_1^\uparrow \leq \nu_2^\uparrow \leq \nu_3^\uparrow \dots, \quad r_1^\downarrow \geq r_2^\downarrow \geq r_3^\downarrow \dots, \quad (24)$$

where in (24) [cf. (21)] the ordered (anti-ordered) eigenvalues of \hat{n} (ρ) refer to the final state in (14). We visualize the orderings of eigenvalues in the initial state (12, 13):

\hat{n}	0	1	2	3	...
	(0, 0)	(0, 1), (1, 0)	(0, 2), (1, 1), (2, 0)	(0, 3), (1, 2), (2, 1), (3, 0)	...
ρ	1	y^α, y	$y^{2\alpha}, y^{\alpha+1}, y^2$	$y^{3\alpha}, y^{2\alpha+1}, y^{\alpha+2}, y^3$...

(25)

where $y \equiv e^{-\beta\omega_1}$. The first, second and third row in (25) show the eigenvalues of (resp.) \hat{n} , (\hat{n}_1, \hat{n}_2) and ρ , with the prefactor ξ is omitted; cf. (12). The unitary process (14, 23) permutes the eigenvalues of ρ . Using (25) one calculates averages of \hat{n} and $\hat{n}_i = a_i^\dagger a_i$:

$$\begin{aligned} \langle \hat{n} \rangle &= \xi (1y^\alpha + 1y + 2y^{2\alpha} + 2y^{\alpha+1} + 2y^2 + \dots), \\ \langle \hat{n}_1 \rangle &= \xi (0y^\alpha + 1y + 0y^{2\alpha} + 1y^{\alpha+1} + 2y^2 + \dots), \\ \langle \hat{n}_2 \rangle &= \xi (1y^\alpha + 0y + 2y^{2\alpha} + 1y^{\alpha+1} + 0y^2 + \dots). \end{aligned} \quad (26)$$

The eigenvalues of ρ in (25) are organized in columns. Whenever the maximal element $y^{k\alpha}$ of k 'th column is larger than the minimal element y^l of l 'th column ($l < k$), we interchange them and achieve some cooling. Formally, we should iterate till all elements in the third row are arranged in descending order; cf. (24). Thus the optimal cooling increases the probability of eigenstates of \hat{n} with lower photon number. Note from (25, 26) that we can interchange elements within each column without changing Δn . The descending order of eigenvalues of ρ in the final state achieves, for a fixed Δn , simultaneously the minimal value of Δn_1 and the maximal value of Δn_2 . This is because the eigenvalues of \hat{n}_1 (\hat{n}_2) in (25) are arranged in ascending (descending) order. Eqs. (16, 18) show that thereby also η and K reach their maximal values at the optimal Δn . The rule (26) stays intact and can be used after permutations.

The exact calculation of (23) is out of reach, since ρ has an infinite number of eigenvalues. But we can develop a useful bound for it by focusing on permutations between nearest-neighbour columns. Define $m \equiv \lceil \frac{\alpha}{1-\alpha} \rceil$, where $\lceil c \rceil$ is the smallest integer $\geq c$. Looking at (25) it is seen that for $k \geq m$, the maximal element of the $(k+1)$ 'th column is larger than the minimal element of k 'th column. Permuting them will contribute to Δn calculated via (23). Likewise, for $k \geq m+2$, the next to maximal element of the $(k+1)$ 'th column is larger than the next to minimal element of k 'th column. To visualize this situation consider a part of (25) between columns $m+p$ and $m+p+1$ ($p \geq 0$):

$$\hat{n} \left\| \begin{array}{c|c} m+p & m+p+1 \\ \hline \rho & \dots, y^{\alpha+m+p-1}, y^{m+p} \mid y^{(m+p+1)\alpha}, y^{(m+p)\alpha+1}, \dots \end{array} \right. \quad (27)$$

where we omitted the second row of (25). Continuing this logic, we see that a new permutation appears for each even p , and that we can cover all nearest-neighbor permutations. Hence a bound [cf. (12, 23)]:

$$0 < -\Delta n_{\text{opt}} \equiv \sum_{k=0}^{\infty} (n_k r_k - \hat{n}_k^\uparrow r_k^\downarrow) \geq \xi \sum_{l=0}^{\infty} y^{l(\alpha+1)} \times \sum_{k=m}^{\infty} (y^{(k+1)\alpha} - y^k) = \frac{(1-y)y^{\alpha(m+1)} - (1-y^\alpha)y^m}{1-y^{\alpha+1}} \quad (28)$$

Cooling is possible for any $0 \leq \alpha < 1$, i.e. (28) is positive and grows with $y = e^{-\beta\omega_1}$ changing from 0 (at $y = 0$) to $\frac{1-\alpha}{1+\alpha}$ at $y = 1$. For $m \gg 1$ the bound (28) gets small, and becomes nearly exact, since the relative error between Δn_{opt} and (28) scales as $\mathcal{O}(y^{2m})$. This estimate follows from the contribution of next to nearest-neighbor permutations and is confirmed in §2 of [27], where we provide further details on the optimal cooling set-up. We report here the limiting values of K and η only, which are obtained as described above [cf. (16, 18, 19)]:

$$\alpha \rightarrow 1 : \quad K_{\text{opt}} \rightarrow \infty, \quad \eta_{\text{opt}} \rightarrow 0, \quad (29)$$

$$\alpha \rightarrow 0 : \quad K_{\text{opt}} \rightarrow \infty, \quad \eta_{\text{opt}} \rightarrow 1, \quad (30)$$

where $\alpha = \omega_2/\omega_1 \rightarrow 0$ in (30) is understood in the sense of a large ω_1 and a small ω_2 . In the last limits of (29, 30) η coincides with Carnot bound. In both limits the energy costs of cooling are negligible: $K_{\text{opt}} \rightarrow \infty$. In the more general case of large ω_1 large and fixed ω_2 , we studied η_{opt} and K_{opt} in §3 of [27].

Feasible interaction Hamiltonian for cooling. How is a permutation unitary U_{opt} realized [28]? Any Hamiltonian that is a polynomial of a fixed degree over a_1, a_1^\dagger, a_2 and a_2^\dagger can be realized via sufficiently many linear operations plus a single-mode non-linearity [29]. However, realizing the permutation U_{opt} should be difficult in practice, since it refers to a Hamiltonian that is a highly non-linear over a_1, a_1^\dagger, a_2 and a_2^\dagger . Hence we focus on a feasible non-linear interaction and determine its cooling ability. The feasibility comes at a cost: now cooling will be possible mostly next to nonlinear resonances: $\omega_2 \gtrsim 2\omega_1$ or $2\omega_2 \lesssim \omega_1$.

The simplest χ^2 nonlinear interactions are realized in an anisotropic (e.g. crystalline) medium and come from the medium polarization \vec{P} being quadratic in electric field \vec{E} [21, 30, 31]: $\vec{P} = \chi^{(1)}\vec{E} + \vec{E}\chi^{(2)}\vec{E}$, where $\chi^{(1)}$ and $\chi^{(2)}$ are susceptibilities. Neglecting polarization, the quantum operator representation of the electric field is $\vec{E} \rightarrow a^\dagger + a$ [31]. Hence the simplest two-mode non-linear interaction Hamiltonian reads:

$$H_I = (a_1^\dagger + a_1)(a_2^\dagger + a_2)^2 + (a_1^\dagger + a_1)^2(a_2^\dagger + a_2), \quad (31)$$

with the full Hamiltonian of the system being

$$H = \omega_1 a_1^\dagger a_1 + \omega_2 a_2^\dagger a_2 + gH_I = H_0 + gH_I \quad (32)$$

where g is the interaction constant. To employ (31, 32) in (15) we introduce the free Heisenberg interaction Hamiltonian $H_I(t) = e^{iH_0 t} H_I e^{-iH_0 t}$ and represent $\rho(t) = e^{-itH} \rho e^{itH}$ in (14) via chronological exponent $\overleftarrow{\mathcal{E}}$

$$\rho(t) = e^{-iH_0 t} \tilde{U} \rho \tilde{U}^\dagger e^{iH_0 t}, \quad \tilde{U} = \overleftarrow{\mathcal{E}}^{-i} \int_0^t ds gH_I(s). \quad (33)$$

Now expand \tilde{U} into Dyson series

$$\begin{aligned} \tilde{U} &= 1 - ig \int_0^t ds H_I(s) \\ &\quad - g^2 \int_0^t ds_1 \int_0^{s_1} ds_2 H_I(s_1) H_I(s_2) + \dots \end{aligned} \quad (34)$$

Using $e^{iH_0 s} a_k e^{-iH_0 s} = e^{-i\omega_k s} a_k$ ($k = 1, 2$) in $H_I(t)$, one can show that the order of magnitude estimate of the k 'th term in (34) reads

$$g^k \Omega^{-k} \sin^k(\Omega t/2), \quad (35)$$

$$\Omega = \min[\omega_1, \omega_2, |2\omega_1 - \omega_2|, |2\omega_2 - \omega_1|]. \quad (36)$$

Thus, for a suitable g , ω_1 and ω_2 we can keep in (34) the first three terms. Within this weak-coupling approximation we calculated (15) in §4 of [27] showing

that sufficiently large cooling $\Delta n < 0$ is possible only for $\omega_2 \gtrsim 2\omega_1$ or $2\omega_2 \lesssim \omega_1$, i.e. for two possible near-resonance conditions. Restricting ourselves with the latter case $\alpha \equiv \omega_2/\omega_1 \lesssim 0.5$ we note that terms $a_1 a_2^{\dagger 2} + a_1^\dagger a_2^2$ in (31) oscillate much slower than other terms. Hence within the rotating wave approximation we can take in (31):

$$H_I \simeq \overline{H}_I \equiv a_1 a_2^{\dagger 2} + a_1^\dagger a_2^2. \quad (37)$$

The approximation is studied in §4 of [27], where we also work out (31). Now \overline{H}_I in (37) leads to an exact operator conservation:

$$2\hat{n}_1 + \hat{n}_2 = \text{const}, \quad \hat{n}_k = a_k^\dagger a_k, \quad k = 1, 2. \quad (38)$$

This conservation is the Manley-Rowe theorem for the considered nonlinear system [20, 21]. The theorem does not generally hold for the complete interaction Hamiltonian (31). However, the cooling necessitates $\alpha \lesssim 0.5$ (or $\alpha \gtrsim 2$) and is accompanied by an approximate conservation law (38) (or $\hat{n}_1 + 2\hat{n}_2 = \text{const}$). Using (37, 38) we get from (34, 33, 15) keeping there the first three terms only (the order of g^2):

$$\begin{aligned} \Delta n_1 &= \frac{8g^2 \sin^2\left(\frac{(2\omega_2 - \omega_1)t}{2}\right)}{(2\omega_2 - \omega_1)^2} \frac{(e^{\beta\omega_1} - e^{2\beta\omega_2})}{(e^{\beta\omega_1} - 1)(e^{\beta\omega_2} - 1)^2}, \\ \Delta n_2 &= -2\Delta n_1, \quad \Delta n = -\Delta n_1, \end{aligned} \quad (39)$$

Hence the cooling at $\alpha \lesssim 0.5$ is described via $\eta = \frac{1}{3}$ and $K = \frac{1}{1-2\alpha}$; cf. (16, 18). Once η is finite and K is large, we achieve cooling with a small energy cost.

Summary. Our starting point was that linear transformations on boson modes (linear optics) increase the overall mean photon number, provided that the initial state is diagonal; see (8). In several senses this is related to increasing the overall noise in the system (though its subsystems can get a noise reduction, as e.g. happen in squeezing [23]). This trend can be overcome only by nonlinear processes, and once we restrict ourselves with feasible processes (e.g. χ^2) on two modes with different frequencies ω_1 and ω_2 , then this cooling in terms of the mean photon number happens in the vicinity of nonlinear resonances. We also studied the optimal cooling, which is possible for any $\omega_1 \neq \omega_2$, but is demanding from the viewpoint of dynamic realization. The cooling is characterized by efficiency and coefficient of performance (COP). The former holds Carnot's bound of the heat-engine efficiency with temperatures replaced by frequencies. For the COP we anticipated, but so far did not identify, a general relation similar to Carnot's bound for the refrigeration COP [19].

We are grateful to Karen Hovhannisyan for important remarks and to David Petrosyan for discussions. This work was supported by SCS of Armenia, grant No. 20TTAT-QTa003.

-
- [1] M. Sheik-Bahae and R. I. Epstein, *Nature Photonics* **1**, 693 (2007).
- [2] A. Abragam and M. Goldman, *Reports on Progress in Physics* **41**, 395 (1978).
- [3] A. B. E. B. Stuart, B. Gal-Or, ed., *A Critical Review of Thermodynamics* (Mono Book Corporation, New York, 1970).
- [4] G. Mahler, *Quantum thermodynamic processes: Energy and information flow at the nanoscale* (CRC Press, 2014).
- [5] R. Silva, G. Manzano, P. Skrzypczyk, and N. Brunner, *Physical Review E* **94**, 032120 (2016).
- [6] H. Wilming and R. Gallego, *Physical Review X* **7**, 041033 (2017).
- [7] F. Clivaz, R. Silva, G. Haack, J. B. Brask, N. Brunner, and M. Huber, *Physical review letters* **123**, 170605 (2019).
- [8] N. Freitas, R. Gallego, L. Masanes, and J. P. Paz, in *Thermodynamics in the Quantum Regime* (Springer, 2018) pp. 597–622.
- [9] S. Raeisi, *Physical Review A* **103**, 062424 (2021).
- [10] D. Gelbwaser-Klimovsky, W. Niedenzu, and G. Kurizki, *Advances In Atomic, Molecular, and Optical Physics* **64**, 329 (2015).
- [11] R. Uzdin, A. Levy, and R. Kosloff, *Physical Review X* **5**, 031044 (2015).
- [12] P. Liuzzo-Scorpo, L. A. Correa, R. Schmidt, and G. Adesso, *Entropy* **18**, 48 (2016).
- [13] R. Long and W. Liu, *Physica A: Statistical Mechanics and its Applications* **443**, 14 (2016).
- [14] J. Gonzalez-Ayala, A. Medina, J. Roco, and A. C. Hernández, *Physical Review E* **97**, 022139 (2018).
- [15] V. Singh, T. Pandit, and R. S. Johal, *Physical Review E* **101**, 062121 (2020).
- [16] S. Raeisi and M. Mosca, *Physical review letters* **114**, 100404 (2015).
- [17] P. Taranto, F. Bakhshinezhad, A. Bluhm, R. Silva, N. Friis, M. P. Lock, G. Vitagliano, F. C. Binder, T. Debarba, E. Schwarzthans, *et al.*, arXiv preprint arXiv:2106.05151 (2021).
- [18] A. E. Allahverdyan, K. V. Hovhannisyan, D. Janzing, and G. Mahler, *Physical Review E* **84**, 041109 (2011).
- [19] A. E. Allahverdyan, K. Hovhannisyan, and G. Mahler, *Physical Review E* **81**, 051129 (2010).
- [20] M. T. Weiss, *Proc. IRE* **45**, 1012 (1957).
- [21] L. Landau and E. Lifshitz, *Electrodynamics of continuous media*, Vol. 8 (Elsevier, 2013).
- [22] C. M. Caves, *Physical Review D* **26**, 1817 (1982).
- [23] J. Garrison and R. Chiao, *Quantum optics* (OUP Oxford, 2008).
- [24] Where these additional photons come from? Answering this question is contingent on realization of the linear transformation; e.g. they come from the medium [23].
- [25] K. V. Hovhannisyan, F. Barra, and A. Imparato, *Physical Review Research* **2**, 033413 (2020).
- [26] A. W. Marshall and I. Olkin, *Inequalities: theory of majorization and its applications* (Academic Press, NY, 1979).
- [27] Supplementary Material contains the following chapters. §1 Numerical results for the optimal cooling. §2 Asymptotic results for the optimal cooling for $\alpha \rightarrow 1$. §3 Asymptotic results for the optimal cooling for $\alpha \rightarrow 0$. §4 Perturbative treatment of the full nonlinear Hamiltonian.
- [28] R.-B. Wu, C. Brif, M. R. James, and H. Rabitz, *Physical Review A* **91**, 042327 (2015).
- [29] S. Lloyd and S. L. Braunstein, in *Quantum information with continuous variables* (Springer, 1999) pp. 9–17.
- [30] G. New, *Introduction to nonlinear optics* (Cambridge University Press, 2011).
- [31] M. Hillery, arXiv preprint arXiv:0901.3439 (2009).

Supplementary Material for
Photon cooling: linear vs nonlinear interactions,
by A. Hovhannisyian, V. Stepanyan and A.E. Allahverdyan

§1 Numerical results for the optimal cooling

Recall our discussion after (25) of the main text. There we explained that the optimal cooling—with respect to all involved quantities Δn_{opt} (photon number difference), K_{opt} (COP or coefficient of performance) and η_{opt} (efficiency)—is achieved once all eigenvalues of the final density matrix are arranged in the descending order; see the third row in (25) of the main text. Numerically, this means that we need to take a sufficiently long but a finite sequence of eigenvalues (starting from the largest one) and ensure that the results are stable with respect to increasing the length of this block.

Our numerical results are shown in Figs. 1, 2 and 3. First, recall that in $K = -\frac{\Delta n_1 + \Delta n_2}{\Delta n_1 + \alpha \Delta n_2}$, the achieved photon number decrease $\Delta n = \Delta n_1 + \Delta n_2 < 0$ is divided over the dimensionless energy cost $\Delta n_1 + \alpha \Delta n_2$; cf. (16) of the main text. It is seen from Fig. 1 that K_{opt} as a function of α has (singular) local minima at points $\alpha = \frac{k}{k+1}$ where $k \in \mathbb{N}$ is an integer. We checked that these local minima of K come mostly from the singular behavior of the energy cost $\Delta n_1 + \alpha \Delta n_2$; see Fig. 2. Now Δn (not shown in figures) shows weak singularities at those points $\alpha = \frac{k}{k+1}$, but these singularities are much weaker than those of the energy cost $\Delta n_1 + \alpha \Delta n_2$.

The origin of these singularities for K_{opt} (and $\Delta n_1 + \alpha \Delta n_2$) can be clarified as follows. Recall that

$$m \equiv \left\lceil \frac{\alpha}{1 - \alpha} \right\rceil, \quad (40)$$

refers to the the group of eigenvalues of the initial state ρ starting from which the eigenvalues of ρ are not arranged in the descending order; see the discussion after (25) of the main text. At points $\alpha = \frac{k}{k+1}$ the index of the block from which the permutations start undergoes a jump discontinuity of increasing by one.

Fig. 3 presents the numerical behavior of η_{opt} as a function of α . It is seen that η_{opt} also shows singularities at $\alpha = \frac{k}{k+1}$, though these singularities are weaker than those for K_{opt} ; cf. Fig. 1. In particular, these singularities do not change the monotonous behavior of η_{opt} as a function of α .

§2 Asymptotic results for the optimal cooling: The limit $\alpha \rightarrow 1$

Eq. (28) of the main text provides the nearest-neighbour approximation for Δn . There we also indicated that (28) of the main text becomes close to its exact

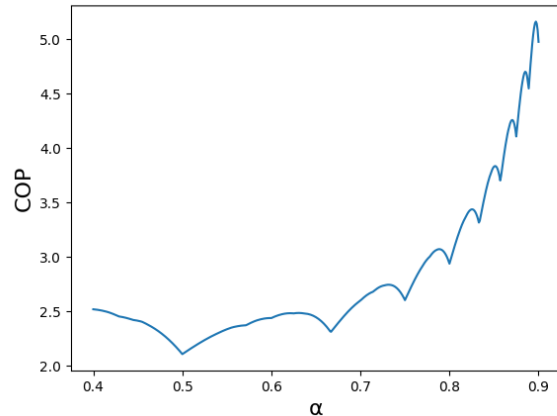


FIG. 1. The coefficient of performance (COP) K_{opt} versus $\alpha = \omega_2/\omega_1 < 1$ for the optimal cooling. Here $y^\alpha = e^{-\beta\omega_2} = 0.6$ and numerical calculations are done up to the block number 300; see (25) of the main text.

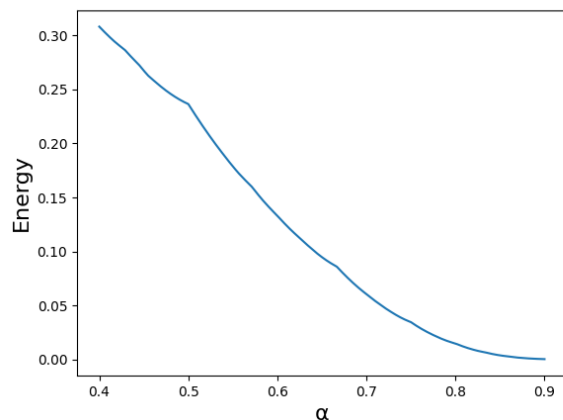


FIG. 2. The same as in Fig. 1, but for the optimal dimensionless energy cost $\Delta n_1 + \alpha \Delta n_2$ versus α .

value whenever m defined via (40) is sufficiently large, or, equivalently $\alpha \rightarrow 1$. The precision of this approximation relates to the necessity of next-nearest-neighbour permutations. The largest value of p in (27) of the main text, where such permutations are necessary can be estimated from the following diagram:

$$\begin{array}{c|c|c|c} \hat{n} & 2m & 2m+1 & 2m+2 \\ \rho & \dots, y^{2m} & \dots & y^{(2m+2)\alpha}, \dots \end{array} \quad (41)$$

Now note from (40) that $y^{2m} < y^{(2m+2)\alpha}$, i.e. a next-nearest-neighbor permutation is necessary. Hence the contribution from next-nearest-neighbor permutation scales as $\mathcal{O}(y^{2m})$, and for $m \gg 1$ this is smaller than what was retained in (28) of the main text. This estimate is crude, since it did not account for permutations that already occurred (within the nearest-neighbor approach)

§2.1 COP in the limit $\alpha \rightarrow 1$

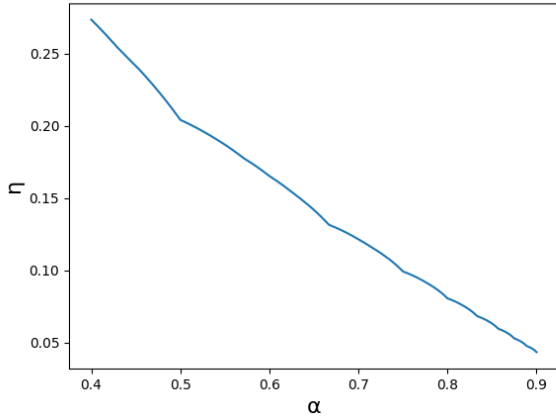


FIG. 3. The same as in Fig. 1, but for the efficiency η_{opt} versus α .

between the columns $2m$ and $2m + 1$. However, it is sufficient for our purposes. Indeed, Fig. 4 shows the relative error of numerically exact calculation of Δn and compares it with (28) of the main text showing that it is well within the above bound $\mathcal{O}(y^{2m})$.

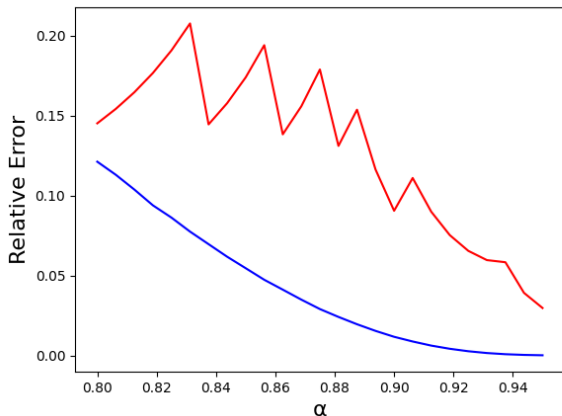


FIG. 4. Here we calculated Δn in numerically exact way by directly arranging all eigenvalues of the final density matrix $\rho(t)$ in the descending order; cf. (25) of the main text. We took $y^\alpha = e^{-\beta\omega_2} = 0.8$ and numerical calculations were done up to block number 100 which is greater than $5m$ [cf. (40)] for all those α values included in the graph. This quantity was denoted by Δn_{exact} . We denote via Δn_{nn} the nearest neighbor approximation given by (28) of the main text.

Blue curve: the relative error $\frac{|\Delta n_{\text{exact}} - \Delta n_{\text{nn}}|}{\Delta n_{\text{nn}}}$. Red curve: $|\frac{y^{2m(\alpha)}}{\Delta n_{\text{nn}}}|$. This curve is kinked, because so is $m(\alpha)$; see (40). It is seen that the relative error is well within the announced range $|\frac{\mathcal{O}(y^{2m(\alpha)})}{\Delta n_{\text{nn}}}|$.

For studying COP K , we can write the mean changes of \hat{n}_1 and \hat{n}_2 in the approximation of nearest-neighbor permutations [cf. (27) of the main text]:

$$\begin{aligned}\Delta n_1 &= \xi \sum_{i=\hat{n}}^{\infty} (y^{\alpha(i+1)} - y^i) \sum_{j=0}^{\infty} y^{j(1+\alpha)} (i+j) \\ \Delta n_2 &= -\xi \sum_{i=\hat{n}}^{\infty} (y^{\alpha(i+1)} - y^i) \sum_{j=0}^{\infty} y^{j(1+\alpha)} (i+j+1),\end{aligned}\quad (42)$$

where $\xi = (1 - e^{-\beta\omega_1})(1 - e^{-\beta\omega_2})$ is the normalization factor; cf. (12) of the main text.

Note that for obtaining (42) we do not make any permutation within columns with the same eigenvalue of \hat{n} ; cf. (25, 47) of the main text. Doing such permutations will make the estimates in (42) closer to the minimal value of Δn_1 and the maximal value of Δn_2 (both for a fixed Δn). Hence (42) suffices for bounding K from below:

$$K \geq \frac{1}{(1-\alpha)(\frac{y^{1+\alpha}}{1-y^{1+\alpha}} + \frac{1}{1-y^\alpha})} \implies \lim_{\alpha \rightarrow 1} K \rightarrow \infty, \quad (43)$$

which is also observed numerically.

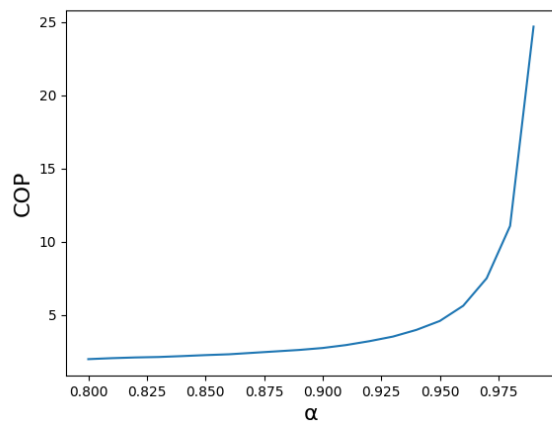


FIG. 5. Numerical results for the coefficient of performance (COP) K . Here $y^\alpha = 0.8$ and numerical calculations are done up to block number $5m$ for all those α values included in the graph.

§3 Asymptotic results for the optimal cooling: The limit $\alpha \rightarrow 0$

§3.1 Error estimation

For α finite and sufficiently close to 0, the action of an optimal unitary results in (44)

$$\frac{N|0\rangle}{R|1\rangle} \left| \begin{array}{c|c|c|c|c} 1 & \dots & a' & & \dots \\ \hline y^\alpha, y^{2\alpha} & \dots, y^{m_1\alpha}, y, y^{(m_1+1)\alpha}, \dots & & & \dots \\ \hline a' + i & & & & \dots \\ \hline y^{(m_2-1)\alpha}, y^2, y^{(m_2+1)\alpha}, y^{(m_2+2)\alpha}, \dots & & & & \dots \end{array} \right|, \quad (44)$$

where $m_1 = \lfloor 1/\alpha \rfloor$, $m_2 = \lfloor 2/\alpha \rfloor \geq 2m_1$, a' is determined from

$$a'(a' + 1)/2 \leq m_1 \leq (a' + 1)(a' + 2)/2 \quad (45)$$

and i from

$$(a' + i)(a' + i + 1)/2 \leq m_2 \leq (a' + i + 1)(a' + i + 2)/2. \quad (46)$$

We see that $i < 3a'$. Now we show that for the calculation of averages of photon numbers one can use

$$\frac{N|0\rangle}{R|1\rangle} \left| \begin{array}{c|c|c|c|c} 1 & 2 & 3 & & \dots \\ \hline y^\alpha, y^{2\alpha} & y^{3\alpha}, y^{4\alpha}, y^{5\alpha} & y^{6\alpha}, y^{7\alpha}, y^{8\alpha}, y^{9\alpha} & & \dots \\ \hline & & & & \dots \end{array} \right|. \quad (47)$$

instead of (44), as in the limit $\alpha \rightarrow 0$ corresponding error terms vanish. We denote by $n_1^{(0)}$ and $n_1^{(*)}$ the average \hat{n}_1 calculated with (44) and (47) respectively, and by Δn_{1e} the error term $n_1^{(0)} - n_1^{(*)}$. Firstly, we write the contribution from the a'^{th} block to the error term

$$\begin{aligned} \Delta n_{1e}^{a'} &= (y - y^{(m_1+1)\alpha})(m_1 + 1 - u) \\ &+ (y^{(m_1+1)\alpha} - y^{(m_1+2)\alpha})(m_1 + 2 - u) + \dots \\ &+ (y^{(u+a'-1)\alpha} - y^{(u+a')\alpha})a', \end{aligned} \quad (48)$$

where $u = a'(a' + 1)/2$. $\Delta n_{1e}^{a'}$ can be estimated from above

$$\begin{aligned} \Delta n_{1e}^{(a')} &\leq (y - y^{(m_1+1)\alpha})a' + (y^{(m_1+1)\alpha} - y^{(m_1+2)\alpha})a' + \\ &+ \dots + (y^{(u+a'-1)\alpha} - y^{(u+a')\alpha})a' = \\ &= (y - y^{(u+a')\alpha})a'. \end{aligned} \quad (49)$$

Similarly, one can estimate the contribution from $(a' + 1)^{\text{th}}$ block

$$\Delta n_{1e}^{(a'+1)} \leq (y^{(u+a')\alpha} - y^{(u+2a'+2)\alpha})(a' + 1). \quad (50)$$

Summing up all contributions we get

$$\begin{aligned} \Delta n_{1e} &\leq [y + y^{(u+a')\alpha} + y^{(u+2a'+2)\alpha} + y^{(u+3a'+5)\alpha} + \dots] \\ &+ [(y^2 - y^{(m_2+1)\alpha})(a' + i) + (y^3 - y^{(m_3+1)\alpha})(a' + i')] \\ &+ (y^4 - y^{(m_4+1)\alpha})(a' + i'') + \dots], \end{aligned} \quad (51)$$

where $m_3 = \lfloor 3/\alpha \rfloor \geq 3m_1$, $m_4 = \lfloor 4/\alpha \rfloor \geq 4m_1$. i' and i'' in (51) are determined from conditions similar to (46):

$$\begin{aligned} \frac{(a' + i')(a' + i' + 1)}{2} &\leq m_3 \leq \frac{(a' + i' + 1)(a' + i' + 2)}{2}, \\ \frac{(a' + i'')(a' + i'' + 1)}{2} &\leq m_4 \leq \frac{(a' + i'' + 1)(a' + i'' + 2)}{2} \end{aligned} \quad (52)$$

and result in $i' < 4a'$ and $i'' < 5a'$. Now, we can estimate (51) further

$$\begin{aligned} \Delta n_{1e} &\leq [y + y^2 + y^3 + y^4 + \dots] \\ &+ [y^2 3a' + y^3 4a' + y^4 5a' + \dots] \leq \\ &\leq \frac{y(1+y)}{1-y} + a' \frac{y \ln y}{(1-y)^2}. \end{aligned} \quad (53)$$

Now, note that in the limit $\alpha \rightarrow 0$, which is $\omega_1 \rightarrow \infty$, a' goes to infinity as $\sqrt{\frac{\omega_1}{\omega_2}}$. As, $0 \leq \Delta n_{1e} \leq \frac{y(1+y)}{1-y} + a' \frac{y \ln y}{(1-y)^2}$ we conclude that (remember that $y = e^{-\omega_1 \beta}$)

$$\lim_{\alpha \rightarrow 0} \Delta n_{1e} \rightarrow 0. \quad (54)$$

§3.2 Asymptotic expressions and their integral representations

In our further calculations we use (47). Using the same procedure as in (26), we find from (47) the following expressions for $\Delta n_{1,2}$ ($\epsilon = \alpha \beta \omega_1$)

$$\begin{aligned} \Delta n_1 &= \xi \sum_{a=0}^{\infty} e^{-\epsilon \frac{a(a+1)}{2}} \sum_{b=0}^a e^{-\epsilon b} b - \xi_1 \sum_a a e^{-\beta \omega_1 a} \\ &= \xi \sum_{a=0}^{\infty} \frac{e^{2\epsilon}}{(e^\epsilon - 1)^2} e^{-\left(\frac{a}{2}+1\right)(a+1)\epsilon} (a(e^{-\epsilon} - 1) + e^{a\epsilon} - 1) \\ &\quad - \frac{1}{e^{\beta \omega_1} - 1}, \\ \Delta n_2 &= \xi \sum_{a=0}^{\infty} e^{-\epsilon \frac{a(a+1)}{2}} \sum_{b=0}^a e^{-\epsilon(a-b)} b - \xi_2 \sum_a a e^{-\epsilon a} \\ &= \xi \sum_{a=0}^{\infty} \frac{e^\epsilon}{(e^\epsilon - 1)^2} e^{-\frac{a(a+1)}{2}\epsilon} (a(e^\epsilon - 1) + e^{-a\epsilon} - 1) \\ &\quad - \frac{1}{e^\epsilon - 1}, \end{aligned} \quad (55)$$

where we defined $\xi_1 = 1 - e^{-\beta \omega_1}$ and $\xi_2 = 1 - e^{-\beta \omega_2}$; hence $\xi = \xi_1 \xi_2$. Before studying (55) numerically, we apply Hubbard-Stratonovich transformation:

$$e^{-\frac{a^2}{2}\epsilon} = \sqrt{\frac{1}{2\pi\epsilon}} \int_{-\infty}^{\infty} dv e^{-\frac{v^2}{2\epsilon} - iav}, \quad (56)$$

for faster and more accurate calculations:

$$\begin{aligned} & \sum_{a=0}^{\infty} e^{-(\frac{a}{2}+1)(a+1)\epsilon} (a(e^{-\epsilon} - 1) + e^{a\epsilon} - 1) \\ &= \sqrt{\frac{1}{2\pi\epsilon}} e^{-\epsilon} \int_{-\infty}^{\infty} dv e^{-\frac{v^2}{2\epsilon}} \left((e^{-\epsilon} - 1) \frac{e^{-(iv+\frac{3}{2}\epsilon)}}{(1 - e^{-(iv+\frac{3}{2}\epsilon)})^2} \right. \\ & \left. + \frac{1}{(1 - e^{-(iv+\frac{1}{2}\epsilon)})} - \frac{1}{(1 - e^{-(iv+\frac{3}{2}\epsilon)})} \right), \end{aligned} \quad (57)$$

$$\begin{aligned} & \sum_{a=0}^{\infty} e^{-\frac{a(a+1)}{2}\epsilon} (a(e^{\epsilon} - 1) + e^{-a\epsilon} - 1) \\ &= \sqrt{\frac{1}{2\pi\epsilon}} \int_{-\infty}^{\infty} dv e^{-\frac{v^2}{2\epsilon}} \left((e^{\epsilon} - 1) \frac{e^{-(iv+\frac{1}{2}\epsilon)}}{(1 - e^{-(iv+\frac{1}{2}\epsilon)})^2} \right. \\ & \left. + \frac{1}{(1 - e^{-(iv+\frac{3}{2}\epsilon)})} - \frac{1}{(1 - e^{-(iv+\frac{1}{2}\epsilon)})} \right). \end{aligned} \quad (58)$$

The results of numerical calculations for η and K are depicted in Fig. 6 and Fig. 7. As seen from figures, $K \rightarrow \infty$ and $\eta \rightarrow 1$ in the limit $\epsilon \ll 1$. Below, we show analytically, that indeed, K and η reach these limits.

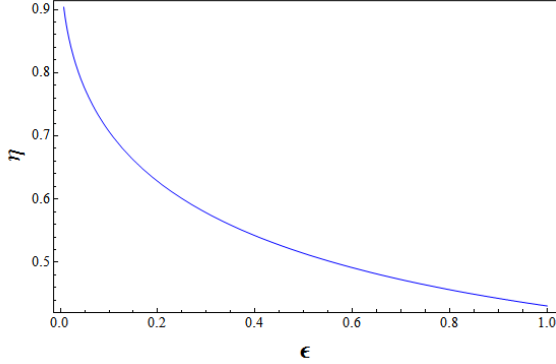


FIG. 6. Numerically calculated efficiency (η) versus ϵ in the limiting case $\omega_1 \gg \omega_2$ using (57) and (58). Here, we set $\beta\omega_1 = 10$ and the smallest value of ϵ is 0.007.

§3.3 Asymptotic results via the Euler-Maclaurin formula

To study the asymptotics of η and K in the limit $\epsilon \ll 1$ we apply the Euler-Maclaurin formula for the sums in

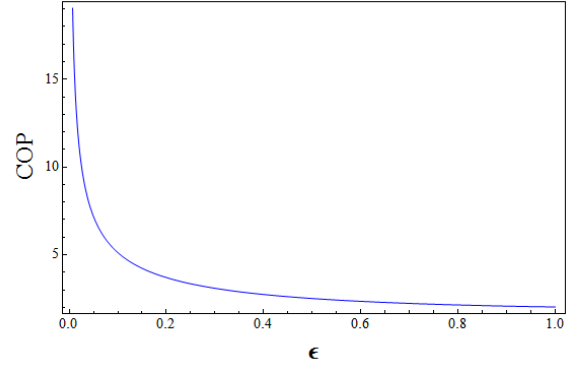


FIG. 7. The same as in Fig. 6 but for COP (K).

$$\begin{aligned} & (55) \\ & \sum_{a=0}^{\infty} \frac{e^{2\epsilon}}{(e^{\epsilon} - 1)^2} e^{-(\frac{a}{2}+1)(a+1)\epsilon} (a(e^{-\epsilon} - 1) + e^{a\epsilon} - 1) \\ & \equiv \sum_{a=0}^{\infty} f_1(a) = \int_0^{\infty} dx f_1(x) + I_1 = S_1 + I_1 \end{aligned} \quad (59)$$

where

$$\begin{aligned} I_1 &= \frac{f_1(0) + f_1(\infty)}{2} \\ &+ \sum_{k=1}^{\lfloor \frac{p}{2} \rfloor} \frac{B_{2k}}{(2k)!} \left(f_1^{(2k-1)}(\infty) - f_1^{(2k-1)}(0) \right) + R_p, \end{aligned} \quad (60)$$

$$R_p \leq \frac{2\zeta(p)}{(2\pi)^p} \int_0^{\infty} dx |f_1^{(p)}(x)|, \quad (61)$$

B_{2k} are Bernoulli numbers, $\zeta(p)$ is the Riemann's zeta function and $f^{(p)}(x)$ is the p^{th} order differential. p in (59) takes different integer values $p \geq 2$ and we use $p = 2$, because this is the simplest case amenable to estimates. Similarly,

$$\begin{aligned} & \sum_{a=0}^{\infty} \frac{e^{\epsilon}}{(e^{\epsilon} - 1)^2} e^{-\frac{a(a+1)}{2}\epsilon} (a(e^{\epsilon} - 1) + e^{-a\epsilon} - 1) \equiv \sum_{a=0}^{\infty} f_2(a) \\ &= \int_0^{\infty} dx f_2(x) + I_2 = S_2 + I_2, \end{aligned} \quad (62)$$

The leading diverging terms in (59) and (62) when $\epsilon \rightarrow 0$ are S_1 and S_2 and we omit I_1 and I_2 . Using (59) and (62) for the efficiency and COP we get the following relations

$$\begin{aligned} K &\approx -\frac{\xi S_1 - n_{1i} + \xi S_2 - n_{2i}}{\xi S_1 - n_{1i} + \alpha(\xi S_2 - n_{2i})}, \\ \eta &\approx -\frac{\xi S_1 - n_{1i} + \xi S_2 - n_{2i}}{\xi S_1 - n_{1i} - \xi S_2 + n_{2i}}, \end{aligned} \quad (63)$$

where n_{1i} and n_{2i} are initial average occupation numbers. The limits $\lim_{\alpha \rightarrow 0} \xi S_{1,2}/n_{2i}$ can be studied analytically, and we get

$$\lim_{\alpha \rightarrow 0} \xi S_{1,2}/n_{2i} = 0.$$

Thus, for the K_{opt} and η_{opt} we obtain

$$K_{\text{opt}} \rightarrow \infty, \quad \eta_{\text{opt}} \rightarrow 1. \quad (64)$$

§4 Perturbative treatment of the full nonlinear Hamiltonian

Let us return to the full—i.e. without the rotating-wave approximation—nonlinear Hamiltonian given by (31) of the main text:

$$H_I = (a_1^\dagger + a_1)(a_2^\dagger + a_2)^2 + (a_1^\dagger + a_1)^2(a_2^\dagger + a_2). \quad (65)$$

See (32) of the main text for the complete Hamiltonian. Here we shall employ (65) in the second-order of Dyson's series given by (34) of the main text; see in this context (33) of the main text. For simplicity we shall scale out the factor β , i.e. we denote $\beta g \rightarrow g$, $\beta \omega_{1,2} \rightarrow \omega_{1,2}$ and $t/\beta \rightarrow t$.

Using (34, 33) of the main text we get

$$\begin{aligned} \text{tr}(\rho(t)\hat{n} - \rho(0)\hat{n}) &= \mathcal{O}(g^3) + g^2 \times \\ &\times \left[\int_0^t ds H_I(s) \hat{n} \int_0^t ds H_I(s) - \right. \\ &- \int_0^t ds_1 \int_0^{s_1} ds_2 H_I(s_1) H_I(s_2) \hat{n} - \\ &\left. - \hat{n} \int_0^t ds_1 \int_0^{s_1} ds_2 H_I(s_2) H_I(s_1) \right]. \end{aligned} \quad (66)$$

Formally the same equation holds for $\hat{n}_k = a_k^\dagger a_k$, where $k = 1, 2$ and $\hat{n} = \hat{n}_1 + \hat{n}_2$.

Substituting (65) into (66) we get

$$\begin{aligned} \Delta n_k &= \text{tr}(\rho(t)\hat{n}_k - \rho(0)\hat{n}_k) = \\ &= g^2 \left[A_k \Phi(\omega_1 + 2\omega_2) + B_k \Phi(\omega_1 - 2\omega_2) + C_k \Phi(\omega_1) \right] + \\ &+ g^2 \left[D_k \Phi(\omega_2 + 2\omega_1) + E_k \Phi(\omega_2 - 2\omega_1) + F_k \Phi(\omega_2) \right], \end{aligned} \quad (67)$$

where $k = 1, 2$,

$$\Phi(x) \equiv \frac{4 \sin^2(\frac{1}{2}xt)}{x^2}, \quad (68)$$

$$\begin{aligned} A_1 &= \frac{2(e^{\omega_1+2\omega_2} - 1)}{(e^{\omega_1} - 1)(e^{\omega_2} - 1)^2}, & A_2 &= \frac{4(e^{\omega_1+2\omega_2} - 1)}{(e^{\omega_1} - 1)(e^{\omega_2} - 1)^2}, \\ B_1 &= \frac{2(e^{\omega_1} - e^{2\omega_2})}{(e^{\omega_1} - 1)(e^{\omega_2} - 1)^2}, & B_2 &= \frac{-4(e^{\omega_1} - e^{2\omega_2})}{(e^{\omega_1} - 1)(e^{\omega_2} - 1)^2}, \\ C_1 &= \frac{4e^{\omega_2}}{(e^{\omega_2} - 1)^2}, & C_2 &= 0. \end{aligned} \quad (69)$$

Now D_1, E_1 and F_1 are obtained from (resp.) A_2, B_2 and C_2 upon swapping ω_1 and ω_2 . Likewise, D_2, E_2 and F_2 are obtained from (resp.) A_1, B_1 and C_1 upon swapping ω_1 and ω_2 .

For a representative pair of frequencies ω_1 and ω_2 , Fig. 8 demonstrates to which extent $\Delta n = \Delta n_1 + \Delta n_2$ calculated via (67) predicts cooling, i.e. $\Delta n < 0$. As announced in the main text, cooling happens in near-resonance conditions $\omega_2 \gtrsim 2\omega_1$ or $2\omega_2 \lesssim \omega_1$, which is seen in Fig. 8; see also Fig. 9 for additional information.

Now the essence of rotating-wave approximation in (67) is that e.g. for $|2\omega_2 - \omega_1| \ll \min[\omega_1, \omega_2, |2\omega_1 - \omega_2|]$, we can take $\Phi(\omega_1 - 2\omega_2)$ in (67) much larger than other terms. This reverts to (39) of the main text.

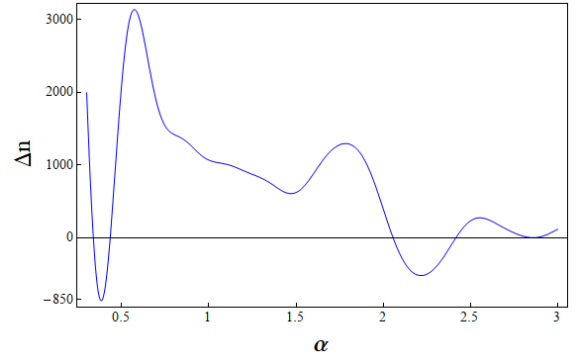


FIG. 8. The photon number difference Δn obtained from (67) and (69) for $\omega_1 = 0.35$ and $t = 10\pi$, where $\alpha = \omega_2/\omega_1$. It is seen that near the resonating frequencies $\alpha \lesssim 0.5$ and $\alpha \gtrsim 2$ the interaction Hamiltonian (65) results in cooling. We see that $\Delta n > 0$ (no cooling) for other values of α .

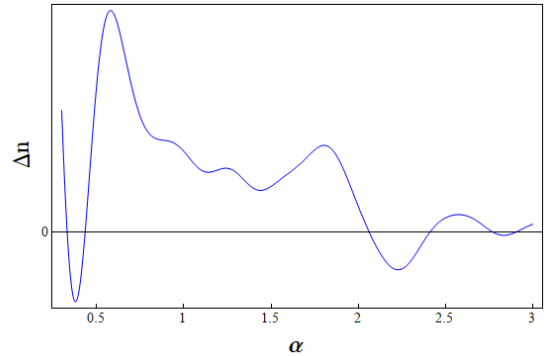


FIG. 9. The photon number difference Δn obtained from (67) and (69) for $\omega_1 = 0.6$ and $t = 6\pi$, where $\alpha = \omega_2/\omega_1$. We see that at the non resonance point $\alpha \approx 2.8$ there are small values of $\Delta n < 0$ (cooling). Hence, although very small, cooling can also be achieved far from the resonance frequencies.

§4.1 Estimation of the higher-order terms in Dyson's series

Using (34) one can show that the terms $\mathcal{O}(g^l)$ in Dyson's series (cf. (66) of the main text) are based on the following structure:

$$\begin{aligned} & \prod_{i=1}^k g \int_0^{s_{i-1}} ds_i H_I(s_i) \times \rho(0) \times \\ & \prod_{i=1}^{k'} g \int_0^{s_{i-1}} ds_i H_I(s_{k'-i+1}) \hat{n}, \end{aligned} \quad (70)$$

where $k + k' = l$ and $s_0 = t$. To get from (70) the term $\mathcal{O}(g^l)$ in Dyson's series we should take the trace of (70) and sum it as $\sum_{k=1, k'=1; k+k=l}^l$.

To study (70), let us take its leftmost multiplier

$$\begin{aligned} & \prod_{i=1}^k g \int_0^{s_{i-1}} ds_i H_I(s_i) = \\ & = \sum_{\alpha_1=1}^8 \dots \sum_{\alpha_k=1}^8 \prod_{i=1}^k g \int_0^{s_{i-1}} ds_i h_{\alpha_i}(s_i). \end{aligned} \quad (71)$$

Here $\{h_i\}_{i=1}^8$ is the set of all monomials in the interaction Hamiltonian (32):

$$\begin{aligned} \{h_i\}_{i=1}^8 = \{ & a_1 a_2^2, a_1^\dagger a_2^2, a_1 a_2^{\dagger 2}, a_1^\dagger a_2^{\dagger 2}, \\ & a_1^2 a_2, a_1^{\dagger 2} a_2, a_1^2 a_2^\dagger, a_1^{\dagger 2} a_2^\dagger \}. \end{aligned} \quad (72)$$

Let us also define the frequency set $\{W_i\}_{i=1}^8$

$$\begin{aligned} \{W_i\}_{i=1}^8 = \{ & \omega_1 + 2\omega_2, -\omega_1 + 2\omega_2, \omega_1 - 2\omega_2, -\omega_1 - 2\omega_2, \\ & 2\omega_1 + \omega_2, -2\omega_1 + \omega_2, 2\omega_1 - \omega_2, -2\omega_1 - \omega_2 \}. \end{aligned} \quad (73)$$

Keeping in mind the equation $a_{1,2}(s) = a_{1,2} e^{-is\omega_{1,2}}$ let us take one term from the sum (71) corresponding to some $\alpha_1 \dots \alpha_k$:

$$\begin{aligned} & \prod_{i=1}^k g \int_0^{s_{i-1}} ds_i h_{\alpha_i}(s_i) = \prod_{i=1}^k g h_{\alpha_i} \times \\ & \times \int_0^{s_{i-1}} ds_i \exp \left[-is_i W_{\alpha_i} \right] = \\ & = \prod_{i=1}^k g h_{\alpha_i} \frac{1}{k!} \prod_{i=1}^k \int_0^t ds_i \exp \left[-is_i W_{\alpha_i} \right]. \end{aligned} \quad (74)$$

The last step uses the fact that we have $k!$ ways to order k different items and that after taking the operator part out of the integration we get integration of complex valued functions which do not change with ordering. Similarly for the rightmost multiplier of (70):

$$\prod_{i=0}^{k'-1} g h_{\alpha'_{k'-i}} \frac{1}{k'!} \prod_{i=1}^{k'} \int_0^t ds_i \exp \left[-is_i W_{\alpha'_i} \right]. \quad (75)$$

Straightforward calculation shows that the integral terms in (74) and (75) result in

$$\prod_{i=1}^k \frac{(1 - e^{-iW_{\alpha_i} t})}{(iW_{\alpha_i})}, \quad \prod_{i=1}^{k'} \frac{(1 - e^{-iW_{\alpha'_i} t})}{(iW_{\alpha'_i})} \quad (76)$$

Now we can write (70) as

$$\begin{aligned} & \sum_{\alpha_1=1}^8 \dots \sum_{\alpha_k=1}^8 \sum_{\alpha'_1=1}^8 \dots \sum_{\alpha'_{k'}=1}^8 \frac{g^k g^{k'}}{k! k'!} \times \\ & \times \left[\prod_{i=1}^k h_{\alpha_i} \prod_{i=0}^{k'-1} h_{\alpha'_{k'-i}} \times \right. \\ & \left. \times \prod_{i=1}^k \frac{(1 - e^{-iW_{\alpha_i} t})}{(iW_{\alpha_i})} \prod_{i=1}^{k'} \frac{(1 - e^{-iW_{\alpha'_i} t})}{(iW_{\alpha'_i})} \right]. \end{aligned} \quad (77)$$

and the equation for $\Delta n_{1,2}$ will be

$$\begin{aligned} \Delta n_{1,2} = & \sum_{k=0}^{\infty} \sum_{k'=0}^{\infty} \delta_{k+k'}^0 \sum_{\alpha_1=1}^8 \dots \sum_{\alpha_k=1}^8 \sum_{\alpha'_1=1}^8 \dots \sum_{\alpha'_{k'}=1}^8 \frac{g^k g^{k'}}{k! k'!} \times \\ & \times \prod_{i=1}^k \frac{(1 - e^{-iW_{\alpha_i} t})}{(iW_{\alpha_i})} \prod_{i=1}^{k'} \frac{(1 - e^{-iW_{\alpha'_i} t})}{(iW_{\alpha'_i})} \times \\ & \times \text{tr} \left(\prod_{i=1}^k h_{\alpha_i} \rho(0) \prod_{i=0}^{k'-1} h_{\alpha'_{k'-i}} \hat{n}_{1,2} \right). \end{aligned} \quad (78)$$

Here the sum $\sum_{\alpha_1=1}^8 \dots \sum_{\alpha_k=1}^8 \sum_{\alpha'_1=1}^8 \dots \sum_{\alpha'_{k'}=1}^8$ will have 8^l elements for any l , so the amount of terms of order $\mathcal{O}(g^l)$ is $8^l(l+1)$. This may put doubt in the claim that the higher order $\mathcal{O}(g^l)$ terms of Δn can be neglected. However, we believe that it can be done because 8^l is a huge overestimation; for most $\alpha_1 \dots \alpha_k, \alpha'_1 \dots \alpha'_{k'}$ the trace

$$\text{tr} \left(\prod_{i=1}^k h_{\alpha_i} \rho(0) \prod_{i=0}^{k'-1} h_{\alpha'_{k'-i}} \hat{n}_{1,2} \right) \quad (79)$$

is zero. Moreover, direct algebraic calculation shows that (79) is nonzero only if the operator

$$\Theta = \prod_{i=1}^k h_{\alpha_i} \prod_{i=0}^{k'-1} h_{\alpha'_{k'-i}} \quad (80)$$

is Hermitian. For example for $l = 2$ from 192 terms we get 18 nonzero terms.